Geochemical Journal, Vol. 55, pp. e25 to e33, 2021 doi:10.2343/geochemj.2.0644

EXPRESS LETTER

High-precision $\Delta'^{17}O$ measurements of geothermal H_2O and MORB on the VSMOW-SLAP scale: evidence for active oxygen exchange between the lithosphere and hydrosphere

TAKASHI SAMBUICHI,[1]* URUMU TSUNOGAI,[1] KAZUSHIGE KURA,[1] FUMIKO NAKAGAWA[1] and TAKESHI OHBA[2]

[1]Graduate School of Environmental Studies, Nagoya University, Nagoya, Aichi 464-8601, Japan
[2]Department of Chemistry, Tokai University, Hiratsuka, Kanagawa 259-1291, Japan

(*Received June 10, 2021; Accepted August 19, 2021; Online published September 14, 2021*)

Recent studies have reported slight but definite differences in $\Delta'^{17}O$ between the lithosphere and hydrosphere. In the present study, we precisely and accurately quantify the $\Delta'^{17}O$ values of geothermal H_2O and mid-ocean ridge basalt (MORB) with normalization on the VSMOW-SLAP scale to further substantiate these differences and to discuss the isotopic evolution of the hydrosphere throughout the geologic time scale. With a $\Delta'^{17}O$ value of $-60 \pm 13 \times 10^{-6}$, the $\Delta'^{17}O$ value of MORB is comparable with that in other silicates reported in previous studies. However, the $\Delta'^{17}O$ value of geothermal H_2O tended to decrease from $+31 \times 10^{-6}$ to -51×10^{-6}, which are the usual $\Delta'^{17}O$ values in meteoric water and silicates, respectively, in accordance with the ^{18}O-enrichment. These results imply an active oxygen isotope exchange between silicates and geothermal H_2O under high-temperature conditions at depth. This is supported by previous studies which report the ^{17}O-enrichment of silicate altered by hydrothermal H_2O. Considering this direct evidence for depletion of ^{17}O, we conclude that the ^{17}O-depleted H_2O has been supplied continuously to the hydrosphere. Additionally, low-temperature interaction between the silicates and H_2O besides high-temperature hydrothermal interaction must be assumed to explain the observed $\Delta'^{17}O$ of the terrestrial hydrosphere. We conclude that the $\Delta'^{17}O$ of the terrestrial hydrosphere should have been variable throughout the geologic time scale owing to the various oxygen exchange interaction between the lithosphere and hydrosphere.

Keywords: triple oxygen isotopes, geothermal H_2O, MORB, VSMOW-SLAP scale, rock-water interaction

INTRODUCTION

Stable isotope ratios of H_2O have provided useful information on the origin of terrestrial H_2O in the global hydrologic cycle. Along with traditional $^2H/^1H$ and $^{18}O/^{16}O$ ratios, recent advances in high-precision measurements of the $\Delta'^{17}O$ [$=\ln(\delta^{17}O+1) - 0.528 \cdot \ln(\delta^{18}O+1)$; detailed in Subsection "Definitions"] of H_2O (Barkan and Luz, 2005; Luz and Barkan, 2010; Steig *et al*., 2014) and silicates (Kim *et al*., 2020; Pack *et al*., 2016; Sharp *et al*., 2016; Tanaka and Nakamura, 2013; Wostbrock *et al*., 2020) have enabled researchers to clarify various geological and geochemical processes such as evolution of the terrestrial hydrosphere and lithosphere throughout the geologic time scale (Herwartz *et al*., 2021; Pack and Herwartz, 2014; Sengupta *et al*., 2020; Sengupta and Pack, 2018; Tanaka and Nakamura, 2013). Many recent studies have reported ^{17}O-depletion in terrestrial silicates compared with that in hydrospheric H_2O such as seawater and meteoric water (Pack *et al*., 2016; Sharp *et al*., 2016). The $\Delta'^{17}O$ value of mantle-derived silicates ranges from -70 to -30×10^{-6}; however, the mean $\Delta'^{17}O$ value of meteoric water is $+33 \times 10^{-6}$ and that of seawater collected at various depths is $-5 \pm 1 \times 10^{-6}$ (Luz and Barkan, 2010).

This difference in $\Delta'^{17}O$ between the lithosphere and hydrosphere has been explained by kinetic fractionation of oxygen isotopes during degassing from the magma ocean on the early primitive earth (Tanaka and Nakamura, 2013) or oxygen isotope exchange between the seawater and lithospheric components such as seafloor basalt and continental crust (Pack and Herwartz, 2014; Sengupta *et al*., 2020; Sengupta and Pack, 2018). The latter explanation has been proposed on the basis of findings that the equilibrium fractionation exponent θ [$=\ln^{17}\alpha/\ln^{18}\alpha$; $^i\alpha_{A\text{-}B} = {}^iR_A/{}^iR_B$ where ^iR corresponds to the abundance ratio of the heavy isotope (^iO where i = 17 or 18) to the light isotope (^{16}O).] between silicates and H_2O is a func-

*Corresponding author (e-mail: tkc.sambuichi@nagoya-u.jp)

Copyright © 2021 by The Geochemical Society of Japan.

tion of temperature (Matsuhisa *et al*., 1978; Sharp *et al*., 2016). Additionally, Pack and Herwartz (2014) proposed that the $\Delta'^{17}O$ of seawater should be variable in accordance with the progress of the oxygen isotope exchange between the seafloor basalt and seawater at various temperatures. Furthermore, Sengupta and Pack (2018) simulated a possible historical evolution of the $\Delta'^{17}O$ of seawater throughout the geologic time scale based on an isotopic mass balance model originally developed by Muehlenbachs and Clayton (1976). Additionally, ^{17}O-depletion in Archean seawater relative to the present value has also been suggested (Sengupta *et al*., 2020).

To verify these hypotheses using oxygen isotope ratios as indicators, the accurate and precise $\Delta'^{17}O$ values of terrestrial H_2O and silicates need to be determined, as does the variation in $\Delta'^{17}O$ of H_2O through interaction of the silicate and H_2O.

The fluorination technique using BrF_5 (Clayton and Mayeda, 1963) has been used to quantitatively convert oxygen in silicates to O_2 and to determine the accurate and precise oxygen isotope ratios of silicates using isotope-ratio mass spectrometry (IRMS). Moreover, the $^{17}O/^{16}O$ and $^{18}O/^{16}O$ ratios of isotopic reference silicates such as NBS28, UWG-2, and San Carlos olivine have been measured relative to Vienna standard mean ocean water (VSMOW) (Kim *et al*., 2020; Pack *et al*., 2016; Sharp *et al*., 2016; Tanaka and Nakamura, 2013; Wostbrock *et al*., 2020) to normalize the oxygen isotope ratios of silicates on the VSMOW scale, which has been used to normalize the oxygen isotope ratios of H_2O in general. However, significant disagreement has been reported on the determined $\Delta'^{17}O$ values of isotopic reference silicates (Pack *et al*., 2016; Sharp *et al*., 2016). To resolve this discrepancy, two-point normalization based on VSMOW and standard light Antarctic precipitation (SLAP) indices has been adopted in recent studies (Kim *et al*., 2020; Pack *et al*., 2016; Sharp *et al*., 2016; Wostbrock *et al*., 2020) following the procedure previously used to normalize oxygen and hydrogen isotope ratios of H_2O in general. Pack *et al*. (2016) determined the $\Delta'^{17}O$ value of San Carlos olivine at two different laboratories based on VSMOW and SLAP. They concluded that normalization onto the VSMOW-SLAP scale reduced the discrepancy among the laboratories. More recently, Khitostrov rock standard (KRS) and Stevns Klint flint standard (SKFS), which were introduced by Miller *et al*. (2020), are also analyzed instead of analyzing VSMOW and SLAP directly to normalize the oxygen isotope ratios of silicate on the VSMOW-SLAP scale (Zakharov *et al*., 2021).

The primary aim of the present study is to precisely determine the $\Delta'^{17}O$ values of high-temperature geothermal H_2O samples and MORB on the VSMOW-SLAP scale to verify the differences in the $\Delta'^{17}O$ between terrestrial silicates and the H_2O in the hydrosphere. Owing to the oxygen isotope exchange between high-temperature geothermal H_2O and silicate (e.g., Giggenbach, 1992), we can expect ^{17}O-depletion in the geothermal H_2O relative to that in the hydrosphere. Because both geothermal H_2O samples and MORB is normalized on the same scale, we can compare them directly with no further corrections required in the values.

Experimental

Definitions

The oxygen isotope ratios are expressed in δ notation:

$$\delta^{i}O = \frac{{}^{i}R_{sample}}{{}^{i}R_{reference}} - 1, \quad (1)$$

where ${}^{i}R$ corresponds to the abundance ratio of the heavy isotope (^{i}O where i = 17 or 18) to the light isotope (^{16}O). Details of the method used for normalization onto the VSMOW-SLAP scale is explained in Section "Results".

The $\Delta'^{17}O$ value is defined by Eq. (2) as

$$\Delta'^{17}O = \delta'^{17}O - \lambda_{RL} \cdot \delta'^{18}O + \gamma_{RL}, \quad (2)$$

where $\delta'^{i}O$ denotes $\ln(\delta^{i}O + 1)$, and λ_{RL} and γ_{RL} denote the slope and the intercept, respectively, of the reference line in the $\delta'^{17}O$-$\delta'^{18}O$ space. Previous studies have adopted various reference lines. In this study, we adopted the reference line which passes the origin ($\gamma_{RL} = 0$) with the slope $\lambda_{RL} = 0.528$. For comparison with the values reported in previous studies, all of previously reported $\Delta'^{17}O$ values were recalculated from the $\delta^{17}O$ and $\delta^{18}O$ values with reference to the definition expressed in Eq. (2) in this study. In addition, both the $\delta^{17}O$ and $\delta^{18}O$ values were rounded to three decimal places to avoid rounding error when calculating the $\Delta'^{17}O$ values.

Samples

The samples of geothermal H_2O including fumarolic condensates were collected from major volcanic and geothermal areas in Japan and were analyzed for both hydrogen and oxygen isotopes (Supplementary Fig. S1 and Supplementary Table S1). The geothermal H_2O were collected directly from natural hot springs. The fumarolic condensates were collected by introducing high-temperature fumarolic gases into two condensation traps soaked in a cold water bath with ice cubes via a quartz or titanium tube inserted into each volcanic fumarole. The location and the temperature during sampling are also shown in Fig. S1 and Table S1. The samples of geothermal H_2O and fumarolic condensates were purified through vaporization and condensation in a vacuum line to remove dissolved reduced components such as sulfides prior to the

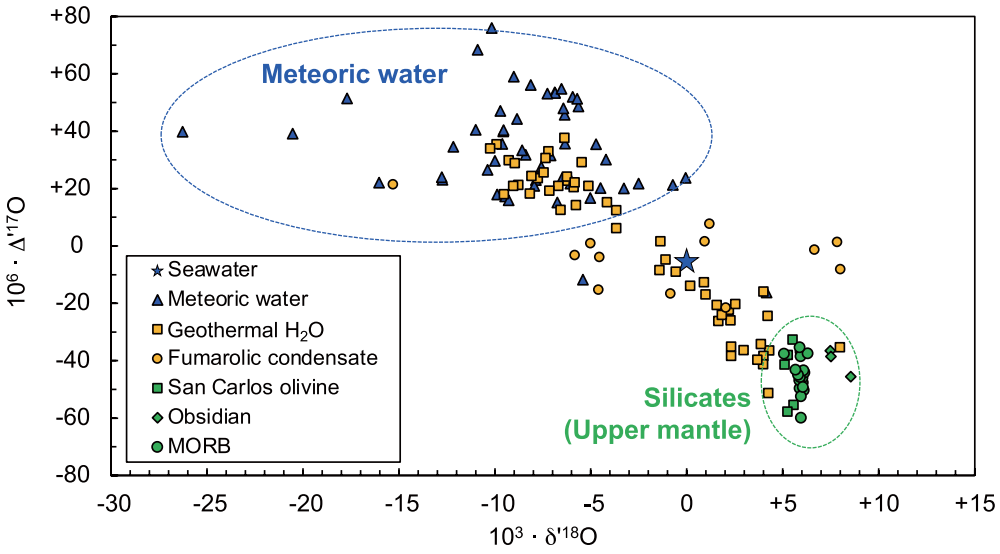

Fig. 1. $\delta'^{18}O$ versus $\Delta'^{17}O$ plot of MORB, geothermal H_2O, and fumarolic condensates determined in this study against those reported in previous studies. The following sources were used to obtain the data: seawater and meteoric water: Luz and Barkan, 2010; San Carlos olivine: Pack et al., 2016; Sharp et al., 2016; Kim et al., 2020; and Wostbrock et al., 2020; obsidian: Greenwood et al., 2018; and Kim et al., 2020; MORB including JFB: Greenwood et al., 2018*; Kim et al., 2020; and this study. *: Correction used San Carlos olivine as the standard assuming that its mean $\delta^{18}O$ and $\Delta'^{17}O$ values coincided with those on the VSMOW-SLAP scale reported in the previous study (+5.32‰ and -52×10^{-6}, respectively; Sharp and Wostbrock, 2021).*

isotope analyses. The changes in $\delta^{18}O$ values through purification were 0.03–0.08‰ for the tap water samples. Because the change values were less than the standard deviation of the $\delta^{18}O$ determination using CRDS, we conclude that the isotopic fractionation owing to purification was negligible.

We also analyzed Juan de Fuca oceanic basalt (JFB) as MORB. The $\delta^{18}O$ and $\Delta'^{17}O$ values of JFB were previously determined to be in the range from +5.33‰ to +5.593‰ and from -64×10^{-6} to -1×10^{-6}, respectively (Ahn *et al.*, 2012; Kim *et al.*, 2019; Kusakabe and Matsuhisa, 2008). The revised values on the VSMOW-SLAP scale were reported recently to be +5.692‰ and -43×10^{-6}, respectively (Kim *et al.*, 2020). Additionally, NBS28, which is a quartz isotope standard distributed by IAEA, was routinely measured to verify the accuracy of our measurement.

Three in-house H_2O standards, ANT, MQ, and CDOW, were prepared and analyzed routinely to obtain accurate $\delta^{17}O$ and $\delta^{18}O$ values of the samples normalized on the VSMOW-SLAP scale. ANT, which is more depleted than the standards in heavy isotopes (^{17}O and ^{18}O), is composed of ice collected in the Antarctic. MQ is ultrapure deionized water made from tap water at Hokkaido University. CDOW, which is more enriched than the others in heavy isotopes (^{17}O and ^{18}O), is commercial desalted Pacific Ocean water ("Marine Gold," Marine Gold Co., Ltd., Muroto, Kochi, Japan) originally collected from offshore area that was concentrated further by distillation at 50°C until the volume was reduced to one-tenth of the original value. The advantage of normalization using these in-house H_2O standards is the relative ease in preparing the standards, of which the $\delta^{17}O$ and $\delta^{18}O$ values are homogeneous and significantly different from each other. Additionally, the normalization ranges can be easily changed depending on the approximate oxygen isotopic compositions in the samples. Although $\delta^{18}O$ value of silicate is typically out of the VSMOW-SLAP range (approximately +5‰ versus VSMOW in $\delta^{18}O$) in general, we can accurately determine the oxygen isotope ratios of silicate using the in-house H_2O standards by interpolation rather than extrapolation (Kim *et al.*, 2020; Pack *et al.*, 2016; Sharp *et al.*, 2016; Wostbrock *et al.*, 2020). In addition to the three in-house H_2O standards, we analyzed Greenland ice sheet precipitation (GISP), which is a H_2O isotope standard distributed by IAEA. The oxygen isotope ratios of all in-house H_2O standards and GISP, were assigned on the basis of direct comparison with VSMOW and SLAP by using a cavity ring-down spectrometer (CRDS; L2140-i with A0211 vaporization module, Picarro Inc., Santa Clara, California, USA) with reference to the method described in Steig *et al.* (2014) (Table 1). The $\delta^{18}O$ value of GISP assigned by IAEA was –24.76‰ (Gonfiantini, 1984).

Measurements on oxygen isotopes

The $\delta^{17}O$ and $\delta^{18}O$ values of the geothermal H_2O and the fumarolic condensates were analyzed using CRDS based on the method proposed by Steig *et al*. (2014). Each sample or standard was measured through 50 injections; only the last 30 injections were used to estimate the mean of the measured isotope ratios to minimize memory effects. The SD for 30 injections of the in-house H_2O standards were 0.022‰ for $\delta^{17}O$, 0.077‰ for $\delta^{18}O$, and 21 × 10^{-6} for $\Delta'^{17}O$. The $\delta^{17}O$ and $\delta^{18}O$ values were normalized on the VSMOW-SLAP scale by using ANT and MQ.

The decomposition of silicates to extract oxygen as O_2 was performed with a conventional fluorination technique using BrF_5 at 500°C. Details of the process are given in Appendix. Conventionally, BrF_5 is used to decompose various types of terrestrial oxygen compounds such as silicates, carbonates, and phosphates, for the measurement on oxygen isotopes. The contribution of the blank O_2, however, was significant during the measurements on silicates in this study. As a result, we corrected the contribution of blank O_2 by the regression analyses (see Section "Results").

In addition, we decomposed three in-house H_2O standards, CDOW, ANT, and MQ, to normalize JFB on the VSMOW-SLAP scale. For this process, we employed the fluorination technique using BrF_5 at 250°C to extract oxygen as O_2.

Extracted and purified O_2 from silicates and in-house H_2O standards, together with the working standard O_2 (Taiyo Nippon Sanso Co., Tokyo, Japan; O_2 purity > 99.99995 vol.%) as the reference gas, was analyzed using the dual inlet mode of a mass spectrometer (Delta V Advantage, Thermo Fisher Scientific Inc., Bremen, Germany) with a cup configuration of m/z = 32, 33, and 34. The m/z = 32 signals were balanced to 2000 ± 50 mV prior to each measurement session. The SD for multiple measurements of NBS28 were 0.046‰ for $\delta^{17}O$, 0.034‰ for $\delta^{18}O$, and 28 × 10^{-6} for $\Delta'^{17}O$.

Normalization onto the VSMOW-SLAP scale

O_2 derived from oxygen compounds other than the samples, such as atmospheric H_2O vapor and trace oxides used in the reaction vessels, that could not be eliminated in the pre-treatment steps prior to the fluorination (blank O_2) could contaminate sample O_2. If such blank O_2 is significant, the measured $\delta^{i}O$ value should change as a function of the sample quantity introduced. During the measurements on the in-house H_2O standards, however, we observed no significant correlation between the $\delta^{i}O$ value relative to the working standard O_2 ($\delta^{i}O_{WG}$) and the reciprocal of the O_2 quantity irrespective of the actual $\delta^{i}O$ value of each in-house H_2O standard ($p > 0.05$), which implies minimum contribution by the blank O_2. Thus, their $\delta^{i}O_{WG}$ values were obtained as the mean of multiple measurements in this study.

From the relation between the $\delta^{i}O_{WG}$ values of the three in-house H_2O standards and their $\delta^{i}O$ values determined on the VSMOW-SLAP scale ($\delta^{i}O_{VSMOW\text{-}SLAP}$), we can relate the $\delta^{17}O_{VSMOW\text{-}SLAP}$ ($\delta^{18}O_{VSMOW\text{-}SLAP}$) values of each sample with $\delta^{17}O_{WG}$ ($\delta^{18}O_{WG}$) values using Eq. (3) [(4)].

$$\delta^{17}O_{VSMOW\text{-}SLAP} = 1.0500 \pm 0.0040 \cdot \delta^{17}O_{WG} + 8.1949 \pm 0.0806 \quad (3)$$

$$\delta^{18}O_{VSMOW\text{-}SLAP} = 1.0563 \pm 0.0041 \cdot \delta^{18}O_{WG} + 16.2352 \pm 0.1557. \quad (4)$$

As clearly represented by the R^2 of 1.0000 (Supplementary Fig. S2) in the equations, we obtained good linear correlation between $\delta^{i}O_{WG}$ and $\delta^{i}O_{VSMOW\text{-}SLAP}$ in a wide isotopic range of more than 55‰ for $\delta^{18}O$. The ranges between –24.7 and +16.1‰ for $\delta^{17}O_{VSMOW\text{-}SLAP}$ and –46.2 to +31.0‰ for $\delta^{18}O_{VSMOW\text{-}SLAP}$ cover the typical oxygen isotope ratios of terrestrial H_2O and silicates, at ≤0‰ for $\delta^{18}O$ and +5 to +10‰ for $\delta^{18}O$, respectively. In this study, we used the equations for normalization of the silicate sample onto the VSMOW-SLAP scale.

A slope of more than 1 indicates that the raw values ($\delta^{i}O_{WG}$) were compressed in the IRMS used in this study. The result further validates that the normalization onto the VSMOW-SLAP scale was required to avoid the disagreement among laboratories on the $\Delta'^{17}O$ values. In addition, the intercepts of +8.195 ± 0.081‰ and +16.235 ± 0.156‰ represent the $\delta^{17}O$ and $\delta^{18}O$ values of our working standard O_2 on the VSMOW-SLAP scale, respectively. The $\Delta'^{17}O$ values of that on the VSMOW-SLAP scale is obtained to be –341 ± 1 × 10^{-6}.

By using fluorination and IRMS for the measurement and Eqs. (3) and (4) for the normalization onto the VSMOW-SLAP scale, we determined the oxygen isotope ratios of GISP to be $\delta^{18}O_{VSMOW\text{-}SLAP}$ = –25.076 ± 0.231‰ and $\Delta'^{17}O_{VSMOW\text{-}SLAP}$ = +18 ± 4 × 10^{-6}. The $\delta^{18}O$ and $\Delta'^{17}O$ values estimated by the fluorination method were slightly lower than those reported in previous studies. However, these values are in agreement with our estimation of GISP based on CRDS ($\delta^{18}O_{VSMOW\text{-}SLAP}$ = –24.664 ± 0.012‰, $\Delta'^{17}O_{VSMOW\text{-}SLAP}$ = +26 ± 3 × 10^{-6}, n = 30) and those obtained by various methodologies such as fluorination with BrF_5 or CoF_3 and the CRDS technique within the error (Supplementary Fig. S3; $p > 0.05$).

RESULTS

The measured $\delta^{17}O$ and $\delta^{18}O$ values of the geothermal H_2O including fumarolic condensates normalized on the VSMOW-SLAP scale are summarized in Supplementary Table S2, together with $\delta^{2}H$ values.

Table 1. Oxygen isotope ratios of in-house H_2O standards and GISP determined using CRDS and normalized on the VSMOW–SLAP scale

Sample	$10^3 \cdot \delta^{17}O$	SD	SEM	$10^3 \cdot \delta^{18}O$	SD	SEM	$10^6 \cdot \Delta'^{17}O$	SD	SEM
ANT	–24.665	0.011	0.002	–46.202	0.066	0.012	+2	13	2
MQ	–5.703	0.016	0.003	–10.823	0.077	0.014	+26	15	3
CDOW	+16.063	0.022	0.004	+30.972	0.071	0.013	–170	21	4
GISP	–13.074	0.016	0.003	–24.664	0.066	0.012	+26	15	3

Supplementary Table S3 summarizes the measured oxygen isotope ratios of JFB normalized on the VSMOW-SLAP scale together with those of NBS28. We found that the $\delta^{18}O$ and $\Delta'^{17}O$ values on the VSMOW-SLAP scale correlated with the reciprocal of O_2 quantities (Supplementary Fig. S4; $p < 0.05$). Additionally, the average O_2 yield of the analyses relative to the theoretical oxygen quantity of each silicate was larger than 100%, which implies that blank O_2 produced through fluorination contributed to the measured O_2. Thus, we conclude that the regression lines represent the mixing lines of O_2 derived from each sample with blank O_2 and that we estimated the oxygen isotope ratios of each sample, from which the contribution of blank O_2 had been corrected, as the intercepts of the regression lines (Fig. S4). The intercepts of $\delta^{18}O_{VSMOW\text{-}SLAP}$ and $\Delta'^{17}O_{VSMOW\text{-}SLAP}$ corresponded to $+5.971 \pm 0.752$‰ and $-60 \pm 13 \times 10^{-6}$; these values agree with the previously reported values of $+5.692 \pm 0.014$‰ and $-43 \pm 1 \times 10^{-6}$, respectively (Kim *et al*., 2020). Additionally, the $\delta^{18}O$ and $\Delta'^{17}O$ values of NBS28 through the same blank correction and the normalization onto the VSMOW-SLAP scale were $+9.740 \pm 0.768$‰ and $-41 \pm 15 \times 10^{-6}$, respectively. Those of NBS28 in this study also agreed with those reported in the previous study normalized on the VSMOW-SLAP scale (+9.57‰ and -50×10^{-6}, respectively; Sharp and Wostbrock, 2021).

The relationships between the values of $\delta'^{18}O$ and $\Delta'^{17}O$ of the samples determined in this study is described in Fig. 1 as are those reported for the mantle-derived silicates, seawater, and meteoric water.

Discussion

$\Delta'^{17}O$ value of JFB

Prior to interpret the $\delta^{18}O$ and $\Delta'^{17}O$ values of geothermal H_2O, we should discuss those of JFB and the isotopic evolution of such volcanic rocks during magmatic processes. The $\delta^{18}O$ and $\Delta'^{17}O$ values of JFB (+5.7 to +6.0‰ and -60 to -43×10^{-6}, respectively; Kim *et al*., 2020; this study) are similar to those of fresh MORB composed of pure glass in which the interactions with seawater were minor (Greenwood *et al*., 2018). The present results imply that the fresh MORB is homogeneous in $\Delta'^{17}O$ within a variation range of 20×10^{-6} regardless of the sampling location (Fig. 1).

Although MORB has a slightly higher $\delta^{18}O$ than the bulk mantle, the $\Delta'^{17}O$ values of the MORB are in good agreement with those of the bulk mantle, represented as San Carlos olivine (Kim *et al*., 2020; Pack *et al*., 2016; Sharp *et al*., 2016; Wostbrock *et al*., 2020). The obsidian, which is felsic volcanic glass precipitated from rhyolitic melt, showed $\delta^{18}O$ values 1–3‰ higher than those of MORB owing to the ^{18}O-enrichment trend from mafic to felsic caused by the crystal differentiation in the melt. Still, the $\Delta'^{17}O$ values of this glass were similar to those of MORB as well.

Neither theoretical nor empirical studies have been conducted thus far to determine the equilibrium fractionation exponent θ ($=\ln^{17}\alpha/\ln^{18}\alpha$) between melt and minerals. However, the empirical θ obtained for the mineral-mineral system, which ranged from 0.528 to 0.529 through magmatic processes under temperatures of 620–1050°C (Pack and Herwartz, 2014), implies that even if the evolution of the mantle-derived melt led to fractionation of $\delta^{18}O$ from those in the upper mantle for 1‰, the $\Delta'^{17}O$ values were almost stable, as evidenced from the θ values close to 0.528 during the oxygen isotope fractionation. We conclude that in general, the $\Delta'^{17}O$ values of $-50 \pm 10 \times 10^{-6}$ represent those of the upper mantle as well as those of fresh volcanic silicates.

$\Delta'^{17}O$ values of geothermal H_2O and fumarolic condensates

The oxygen isotope ratios of geothermal H_2O are shown in the $\delta'^{18}O$-$\Delta'^{17}O$ space together with those reported for meteoric water and silicates (Fig. 1). Although the meteoric water generally showed $\delta^{18}O$ values lower than those of seawater owing to isotope fractionations during evaporation from seawater (e.g., Dansgaard, 1964), the geothermal H_2O showed relative ^{18}O-enrichment from local meteoric water owing to (1) oxygen isotope exchange with silicates or (2) mixing with ^{18}O-enriched magmatic H_2O (e.g., Giggenbach, 1992).

In accordance with the ^{18}O-enrichment, they showed lower $\Delta'^{17}O$ values, from +31 to -51×10^{-6}. The relation can be explained by the mixing of H_2O with lower $\Delta'^{17}O$ values of -40×10^{-6} or less to the local meteoric water (or seawater). Both the $\delta^{18}O$ and $\Delta'^{17}O$ values of the hy-

pothetical H_2O with low $\Delta'^{17}O$ values coincided with those of fresh MORB.

As discussed in previous sections, the terrestrial silicates are characterized by both higher $\delta^{18}O$ and lower $\Delta'^{17}O$ compared with meteoric water and seawater irrespective of the evolution of the silicates from those in the upper mantle. Additionally, under the oxygen isotope exchange equilibrium between silicates and H_2O at temperatures of 300–400°C with high (infinite) rock/water ratio, the $\Delta'^{17}O$ values of H_2O should be close to those of silicate (Sharp *et al*., 2016). Therefore, mixing of H_2O that had been under the oxygen isotope exchange equilibrium with silicates at elevated temperatures is a likely explanation for the lower $\Delta'^{17}O$ values of geothermal H_2O than those of local meteoric water. Another possible explanation for the $\Delta'^{17}O$ values of the geothermal H_2O is the mixing of magmatic H_2O that originated from both the subducted H_2O discharged into the mantle wedge at great depth in the subduction zone and H_2O originally in the upper mantle (e.g., Giggenbach, 1992). Even if that were the case, the $\Delta'^{17}O$ value of this magmatic H_2O should coincide with that of the melt owing to the rapid oxygen isotope exchange between H_2O and silicates under the θ values close to λ_{RL} (=0.528) (Sharp *et al*., 2016).

The δ^2H values of the geothermal H_2O increased in accordance with the ^{18}O-enrichment (Supplementary Fig. S5). Besides to contribution of magmatic H_2O interacted with lithosphere, the isotopic fractionation during phase separation (Craig, 1963) could be responsible for the observed linear relation with the slope lower than the meteoric water line ($\delta^2H = 8 \cdot \delta^{18}O + 10$; Dansgaard, 1964) in the δ^2H-$\delta^{18}O$ space. Because the θ value between vapor and liquid at a temperature of 100°C is likely close to λ_{RL} (Barkan and Luz, 2005; Zakharov *et al*., 2019), it is difficult to explain the ^{17}O-depletion of the geothermal H_2O by the isotopic fractionation during the phase separation of geothermal H_2O. Rather, the contribution of the H_2O interacted with the lithosphere is more reasonable to explain the changes of both δ^2H and $\Delta'^{17}O$ values in accordance with the ^{18}O-enrichment of the geothermal H_2O. Therefore, oxygen with low $\Delta'^{17}O$ values in the lithosphere should be highly responsible for the origin of those with low $\Delta'^{17}O$ values in the geothermal H_2O irrespective of the H_2O's origin. We conclude that oxygen isotope exchange with the lithosphere under elevated temperatures was responsible for the ^{17}O-depletion of the geothermal H_2O.

Implications for the isotopic evolution of the terrestrial hydrosphere

Considering that geothermal H_2O is generally an analog of high-temperature hydrothermal H_2O including deep-sea venting, the present results on geothermal H_2O imply that H_2O with low $\Delta'^{17}O$ was supplied continuously to the terrestrial hydrosphere through oxygen isotope exchange with the lithosphere under high-temperature conditions. Reports of the changes in the $\Delta'^{17}O$ of MORB owing to hydrothermal alteration (Sengupta and Pack, 2018) also support this hypothesis. The oxygen isotope exchange rate between seafloor basalt and seawater is 1.8×10^{13} kg-O/year, as estimated from the volume of the high-temperature altered phase in the seafloor basalt (Muehlenbachs, 1998; Sengupta and Pack, 2018). Thus, approximately 60 times amount of oxygen in the present seawater (1.2×10^{21} kg-O) should have been exchanged between the seafloor basalt and seawater throughout the geologic time scale (4 Ga). Consequently, any possible $\Delta'^{17}O$ in the primitive ocean owing to the kinetic fractionation process (Tanaka and Nakamura, 2013) such as the degassing of H_2O was no longer preserved in the present seawater even if such relative ^{17}O-enrichment occurred. Rather, we must attribute the $\Delta'^{17}O$ of the present seawater to the subsequent interactions between the silicates and seawater. Furthermore, the direct evidence for the continuous supply of the ^{17}O-depleted H_2O into the hydrosphere implies that we must assume low-temperature interactions between the lithosphere and the hydrosphere (Pack and Herwartz, 2014; Sengupta *et al*., 2020; Sengupta and Pack, 2018) to explain the $\Delta'^{17}O$ of the present seawater besides the high-temperature interaction. As a result, this $\Delta'^{17}O$ of H_2O in the hydrosphere should be variable throughout the geologic time scale.

Conclusions

The $\Delta'^{17}O$ values of the geothermal H_2O showed a large variation ranging of –51 to +31 $\times 10^{-6}$. With $\Delta'^{17}O$ values of $-60 \pm 13 \times 10^{-6}$, the $\Delta'^{17}O$ value of JFB, was significantly lower in general than that of seawater and meteoric water. This result coincides with those of mantle-derived silicates reported in previous studies. Additionally, the oxygen isotopes of the geothermal H_2O are plotted on the hypothetical mixing line between mantle-derived silicates and meteoric water (or seawater) in the $\delta'^{18}O$-$\Delta'^{17}O$ space. This implies that the oxygen isotope exchange between silicates and H_2O was responsible for the production of ^{17}O-depleted H_2O in the geothermal H_2O. We conclude that the ^{17}O-depleted H_2O has been supplied continuously into the hydrosphere and that the $\Delta'^{17}O$ of the terrestrial hydrosphere should be variable in response to the interaction between the lithosphere and the hydrosphere throughout the geologic time scale.

Acknowledgments—The authors thank Dr. M. Kusakabe (University of Toyama, Japan) and KOPRI (Korea Polar Research Institute, Incheon, Republic of Korea) for distributing BrF_5 and Juan de Fuca basalt. We also thank Dr. H. Shinohara (Geological Survey of Japan) for coordinating the survey on volcanoes

and providing us geothermal H_2O samples. Additionally, we thank Noboribetsu Onsen Co., Ltd. for providing us geothermal H_2O samples. We would like to thank the anonymous reviewers for constructive comments that helped improve the manuscript.

APPENDIX A

A1. Methodologies

A1.1. Fluorination line The fluorination technique using BrF_5 was applied to decompose the H_2O and silicates into O_2 in this study. This measurement system was newly installed at Nagoya University, Japan. The schematic diagrams of the fluorination line and the reaction vessels used in this study are shown in Supplementary Figs. S6 and S7, respectively. The design of the line follows that used at the Korea Polar Research Institute (Kim *et al*., 2020). Most parts of the line and the reaction vessels were composed of stainless steel tubes, unions, and bellows sealed valves supplied by Swagelok (Solon, Ohio, USA). For storing the BrF_5 and byproducts produced during fluorination, we used custom-made polychlorotrifluoroethylene (PCTFE) Kel-F® tubes that were resistant to fluoride, hydrophobic, and semi-transparent to reveal the inside of the tubes.

The fluorination line consisted of two parts: a distillation line and a purification line (Fig. S6). The distillation line was used to purify the BrF_5 by distillation and to distribute it into a reaction vessel connected to UT 1. The BrF_5 was purified through distillation by using both LN_2 and a dry ice/ethanol mixture prior to use for the fluorination. The purification line was used to extract and purify O_2 from the gases (O_2, residual BrF_5, and byproducts other than O_2) in a reaction vessel connected to UT 2. The line included two cold traps (CT 1 and CT 2) and a chemical trap (KBr trap) filled with KBr particles. A cold sample tube filled with molecular sieve 5A (MS trap) was connected at UT3 for collecting all of the purified O_2 of each sample under the LN_2 temperature.

A1.2. Fluorination and purification of H_2O The reaction vessel used to convert H_2O to O_2 using BrF_5 was a 50 mL stainless steel tube (Fig. S7(a)); a glass tube was used for injection and purification of the H_2O sample. About 2–4 μL of the H_2O sample was subsampled into the glass tube by using a microsyringe and was then frozen at the bottom of the tube using LN_2. Afterward, N_2, Ar, and O_2 in the gas phase were evacuated. The same evacuation procedure was repeated twice more by changing the LN_2 to the dry ice/ethanol mixture to remove the CO_2 and N_2O. Each H_2O sample, sealed in the reaction vessel, was fluorinated using excess BrF_5 at twice the stoichiometrically required amount at 250°C for 1 h.

After the fluorination, all of the O_2 produced in the reaction vessel was introduced into the purification line through UT 2 and was recovered onto the sample tube with molecular sieve 5A under LN_2 temperature. The other byproducts, including residual BrF_5, BrF_3, Br_2, HF, and NF_3, were trapped at CT 1 and CT 2 under LN_2 temperature, and F_2 was trapped at the KBr trap in the line at 150°C.

A1.3. Fluorination and purification of silicate The reaction vessel for silicate (Ni reactor) was composed of nickel and stainless steel (Fig. S7(b)). The bottom 10 cm of the reactor, which was heated during fluorination, was composed of a 1" O.D. nickel tube welded onto a Swagelok vacuum coupling radiation (VCR) gland. This tube was connected to the stainless steel tube with a VCR connector located at the tube′s midpoint. After removing the stainless steel tube from the connector, we loaded each sample into the reactor and removed the (un)reacted residues after fluorination.

About 2–13 mg of JFB was loaded into the Ni reactor. The reactor was evacuated at 150°C for 16 h and at 300°C for 2–4 h. Afterward, the reactor was cooled to 50°C, and a small amount of BrF_5 was expanded into the line and the reactor to remove microcontaminants such as atmospheric H_2O. After 1 h, the expanded BrF_5 was collected into a PCTFE tube under LN_2 temperature, and the residual gases were evacuated. Each silicate was fluorinated at 500°C for 16 h by using excess BrF_5 at three to four times the stoichiometrically required amount. To avoid heating the VCR gasket during the fluorination, a copper tube through which water flowed was installed below the VCR connector. After the fluorination, the O_2 produced in the reactor was purified following the same procedures as those used for the H_2O fluorination and was collected in the sample tube described already.

A1.4. Collection and introduction of O_2 to IRMS To avoid possible changes in the oxygen isotope ratios including $\Delta'^{17}O$ of O_2 owing to incomplete desorption from molecular sieves under room temperature, we used a cryostat system (Iwatani Corporation, Tokyo, Japan) to completely desorb the O_2 from the molecular sieves. This system enabled the O_2 in the sample tube to be introduced into one of the six sample ports cooled to –250°C. After gathering the O_2 into a port for 30 min while heating the sample tube to 60°C, the port was isolated by closing diaphragm valves (SS-DSVCR4, Swagelok, Solon, Ohio, USA) at the inlet of each port. Then, the O_2 in each port was measured after being introduced under room temperature into the pre-evacuated bellows of the IRMS (Delta V Advantage, Thermo Fisher Scientific, Inc., Bremen, Germany) through diffusion.

A2. Data analyses

For calculating the SEM for an intercept and a slope of a linear regression line ($y = \beta x + \alpha$) obtained by the least-squares method, the SEM of each measurement should be propagated to them. According to propagation law of error, these values are expressed as

$$e_f^2 = \sum_{j=1}^{n}\left(\frac{\partial f}{\partial x_j}\cdot e_{x_j}\right)^2 + \sum_{j=1}^{n}\left(\frac{\partial f}{\partial y_j}\cdot e_{y_j}\right)^2, \qquad \text{(A1)}$$

where e and n denote the SEM and number of analyses, respectively, and f denotes an intercept (α) or a slope (β) term, which are functions of x_j and y_j, of the least-squares method. Equation (A1) can be expanded by using the α and α terms of the least-squares method, as shown Eqs. (A2) and (A3), respectively.

$$e_\alpha^2 = \frac{\left\{\left(\sum x_j\right)^2 \cdot \sum x_j^2 - \sum x_j y_j \cdot \sum x_j \cdot \sum y_j\right\}\cdot \sum e_{x_j}^2}{\left\{n\cdot\sum x_j^2 - \left(\sum x_j\right)^2\right\}^2}$$

$$+ \frac{\beta\cdot\sum x_j y_j \cdot \sum e_{x_j}^2 + \sum x_j^2 \cdot \sum e_{y_j}^2}{n\cdot\sum x_j^2 - \left(\sum x_j\right)^2}, \qquad \text{(A2)}$$

$$e_\beta^2 = \frac{\left\{n^2\cdot\sum y_j^2 - n\cdot\left(\sum y_j\right)^2\right\}\cdot\sum e_{x_j}^2}{\left\{n\cdot\sum x_j^2 - \left(\sum x_j\right)^2\right\}^2} + \frac{n\cdot\sum e_{y_j}^2}{n\cdot\sum x_j^2 - \left(\sum x_j\right)^2} \qquad \text{(A3)}$$

In this study, we used these equations to estimate the SEM for the intercepts and the slopes of the normalization equations onto the VSMOW-SLAP scale. For the normalization equations, x and y denote $\delta^{i}O_{WG}$ and $\delta^{i}O_{VSMOW\text{-}SLAP}$ of the in-house H_2O standards, respectively. Additionally, 3 was substituted for n because three in-house H_2O standards were used to obtain the normalization equations.

References

Ahn, I., Lee, J. I., Kusakabe, M. and Choi, B. G. (2012) Oxygen isotope measurements of terrestrial silicates using CO_2-laser BrF_5 fluorination technique and the slope of terrestrial fractionation line. *Geosci. J.* **16**, 7–16.

Barkan, E. and Luz, B. (2005) High precision measurements of $^{17}O/^{16}O$ and $^{18}O/^{16}O$ ratios in H_2O. *Rapid Commun. Mass Spectrom.* **19**, 3737–3742.

Clayton, R. and Mayeda, T. (1963) The use of bromine pentafluoride in the extraction of oxygen from oxides and silicates for isotopic analysis. *Geochim. Cosmochim. Acta* **27**, 43–52.

Craig, H. (1963) The isotope geochemistry of water and carbon in geothermal areas. *Nucl. Geol. Geotherm. Areas* (Tongiorgi, E. ed.), 17–53.

Dansgaard, W. (1964) Stable isotopes in precipitation. *Tellus* **16**, 436–468.

Giggenbach, W. F. (1992) Isotopic shifts in waters from geothermal and volcanic systems along convergent plate boundaries and their origin. *Earth Planet. Sci. Lett.* **113**, 495–510.

Gonfiantini, R. (1984) Stable isotope reference samples for geochemical and hydrological investigations. *Int. J. Appl. Radiat. Isot.* **35**, 426.

Greenwood, R. C., Barrat, J. A., Miller, M. F., Anand, M., Dauphas, N., Franchi, I. A., Sillard, P. and Starkey, N. A. (2018) Oxygen isotopic evidence for accretion of Earth's water before a high-energy Moon-forming giant impact. *Sci. Adv.* **4**.

Herwartz, D., Pack, A. and Nagel, T. J. (2021) A CO_2 greenhouse efficiently warmed the early Earth and decreased seawater $^{18}O/^{16}O$ before the onset of plate tectonics. *Proc. Natl. Acad. Sci.* **118**, e2023617118.

Kim, N. K., Kusakabe, M., Park, C., Lee, J. I., Nagao, K., Enokido, Y., Yamashita, S. and Park, S. Y. (2019) An automated laser fluorination technique for high-precision analysis of three oxygen isotopes in silicates. *Rapid Commun. Mass Spectrom.* **33**, 641–649.

Kim, N. K., Park, C. and Kusakabe, M. (2020) Two-point normalization for reducing inter-laboratory discrepancies in $\delta^{17}O$, $\delta^{18}O$, and $\Delta'^{17}O$ of reference silicates. *J. Anal. Sci. Technol.* **11**.

Kusakabe, M. and Matsuhisa, Y. (2008) Oxygen three-isotope ratios of silicate reference materials determined by direct comparison with VSMOW-oxygen. *Geochem. J.* **42**, 309–317.

Luz, B. and Barkan, E. (2010) Variations of $^{17}O/^{16}O$ and $^{18}O/^{16}O$ in meteoric waters. *Geochim. Cosmochim. Acta* **74**, 6276–6286.

Matsuhisa, Y., Goldsmith, J. R. and Clayton, R. N. (1978) Mechanisms of hydrothermal crystallization of quartz at 250°C and 15 kbar. *Geochim. Cosmochim. Acta* **42**, 173–182.

Miller, M. F., Pack, A., Bindeman, I. N. and Greenwood, R. C. (2020) Standardizing the reporting of $\Delta'^{17}O$ data from high-precision oxygen triple-isotope ratio measurements of silicate rocks and minerals. *Chem. Geol.* **532**, 119332.

Muehlenbachs, K. (1998) The oxygen isotopic composition of the oceanic, sediments and the safloor. *Chem. Geol.* **145**, 263–273.

Muehlenbachs, K. and Clayton, R. N. (1976) Oxygen isotope composition of the oceanic crust and its bearing on seawater. *J. Geophys. Res.* **81**, 4365–4369.

Pack, A. and Herwartz, D. (2014) The triple oxygen isotope composition of the Earth mantle and understanding $\Delta^{17}O$ variations in terrestrial rocks and minerals. *Earth Planet. Sci. Lett.* **390**, 138–145.

Pack, A., Tanaka, R., Hering, M., Sengupta, S., Peters, S. and Nakamura, E. (2016) The oxygen isotope composition of San Carlos olivine on the VSMOW2-SLAP2 scale. *Rapid Commun. Mass Spectrom.* **30**, 1495–1504.

Sengupta, S. and Pack, A. (2018) Triple oxygen isotope mass balance for the Earth's oceans with application to Archean cherts. *Chem. Geol.* **495**, 18–26.

Sengupta, S., Peters, S. T. M., Reitner, J., Duda, J.-P. and Pack, A. (2020) Triple oxygen isotopes of cherts through time. *Chem. Geol*. **554**, 119789.

Sharp, Z. D. and Wostbrock, J. A. G. (2021) Standardization for the tripe oxygen isotope system: Waters, wilicates, carbonates, air, and sulfites. *Rev. Mineral. Geochem*. **86**, 179–196.

Sharp, Z. D., Gibbons, J. A., Maltsev, O., Atudorei, V., Pack, A., Sengupta, S., Shock, E. L. and Knauth, L. P. (2016) A calibration of the triple oxygen isotope fractionation in the SiO_2-H_2O system and applications to natural samples. *Geochim. Cosmochim. Acta* **186**, 105–119.

Steig, E. J., Gkinis, V., Schauer, A. J., Schoenemann, S. W., Samek, K., Hoffnagle, J., Dennis, K. J. and Tan, S. M. (2014) Calibrated high-precision ^{17}O-excess measurements using cavity ring-down spectroscopy with laser-current-tuned cavity resonance. *Atmos. Meas. Tech*. **7**, 2421–2435.

Tanaka, R. and Nakamura, E. (2013) Determination of ^{17}O-excess of terrestrial silicate/oxide minerals with respect to Vienna Standard Mean Ocean Water (VSMOW). *Rapid Commun. Mass Spectrom*. **27**, 385–397.

Wostbrock, J. A. G., Cano, E. J. and Sharp, Z. D. (2020) An internally consistent triple oxygen isotope calibration of standards for silicates, carbonates and air relative to VSMOW2 and SLAP2. *Chem. Geol*. **533**, 119432.

Zakharov, D. O., Bindeman, I. N., Tanaka, R., Fridleifsson, G. Ó., Reed, M. H. and Hampton, R. L. (2019) Triple oxygen isotope systematics as a tracer of fluids in the crust: A study from modern geothermal systems of Iceland. *Chem. Geol*. **530**, 119312.

Zakharov, D. O., Martin-Carbonne, J., Alleon, J. and Bindeman, I. N. (2021) Triple oxygen isotope trend recorded by Precambrian cherts: A perspective from combined bulk and in situ secondary ion probe measurements. *Rev. Mineral. Geochem*. **86**, 323–365.

Supplementary Materials

URL (http://www.terrapub.co.jp/journals/GJ/archives/data/55/MS644.pdf)
Figures S1 to S7
Tables S1 to S3